

Supporting Information to

“Impact of Molecular Weight on Electrochemical Properties of Poly(TEMPO methacrylate).”

Kai Zhang,¹ Yuxiang Hu,^{1,2} Lianzhou Wang,^{1,2} Jiyu Fan,³ Michael J. Monteiro,¹ Zhongfan Jia^{1}*

1. Australian Institute for Bioengineering and Nanotechnology, University of Queensland,
Brisbane QLD 4072, Australia
2. School of Chemical Engineering, University of Queensland, Brisbane QLD 4072, Australia
3. Department of Applied Physics, Nanjing University of Aeronautics and Astronautics,
Nanjing 210016, China

E-mail: z.jia@uq.edu.au (Z.J.).

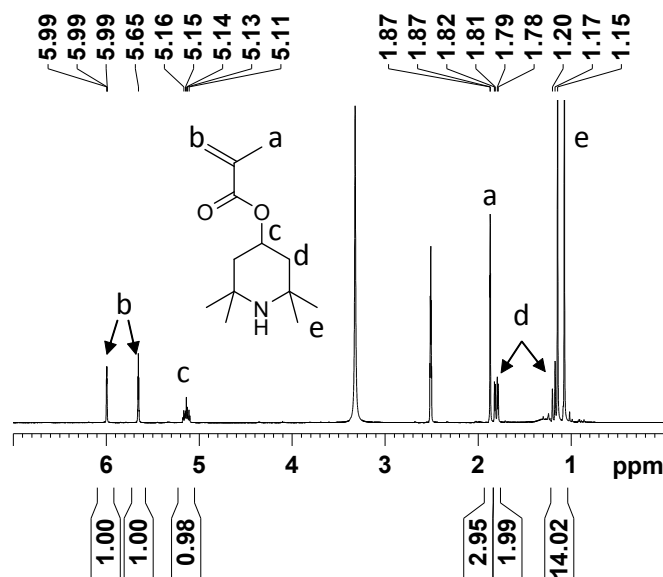


Figure S1. ^1H NMR spectrum (400MHz) of 2,2,6,6-tetramethylpiperidin-4-yl methacrylate (TMMPM) in $\text{DMSO}-d_6$.

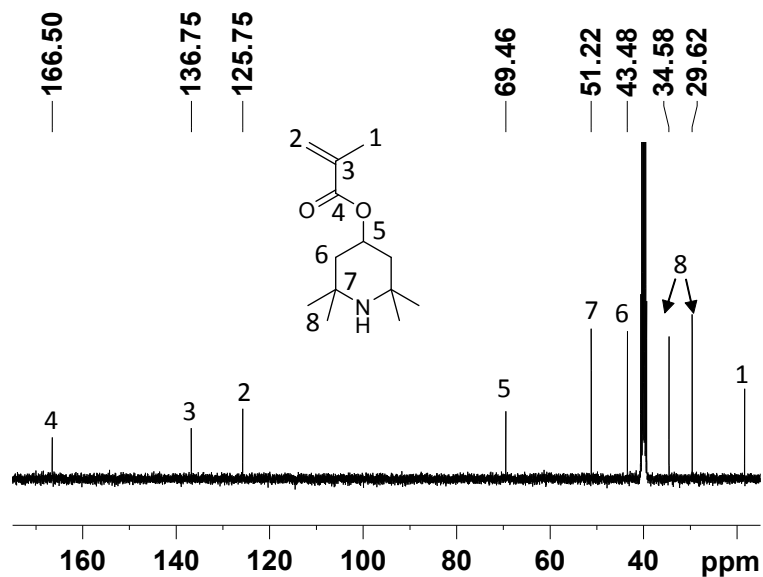


Figure S2. ^{13}C NMR spectrum (100MHz) of 2,2,6,6-tetramethylpiperidin-4-yl methacrylate (TMMPM) in $\text{DMSO}-d_6$.

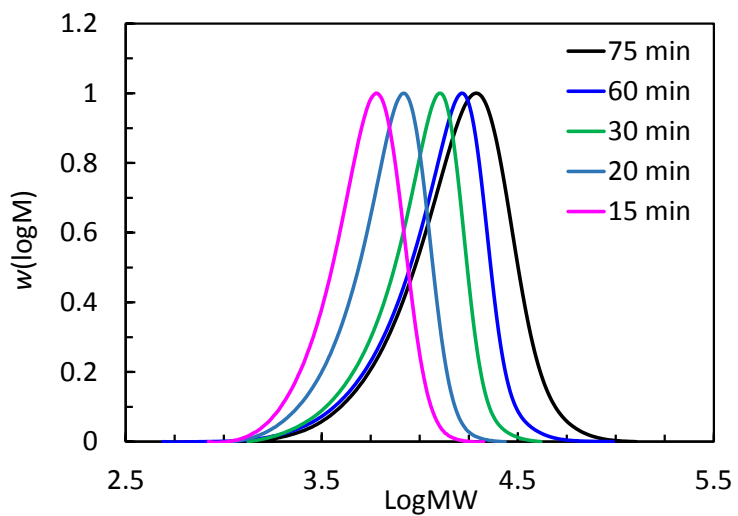


Figure S3. SEC traces of PTMA oxidised from PTMPM by H_2O_2 in methanol, the traces were recorded in THF SEC using polystyrene as standard.

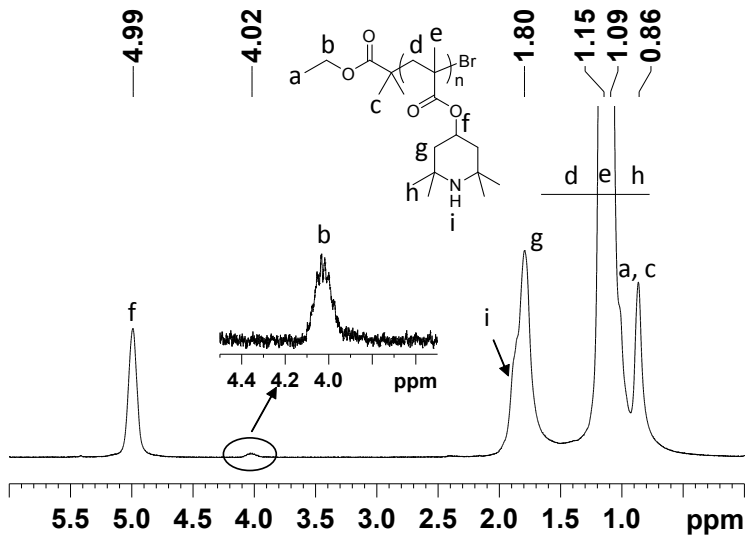


Figure S4. Typical ^1H NMR spectrum (400MHz) of PTMPM_{66} in CDCl_3 .

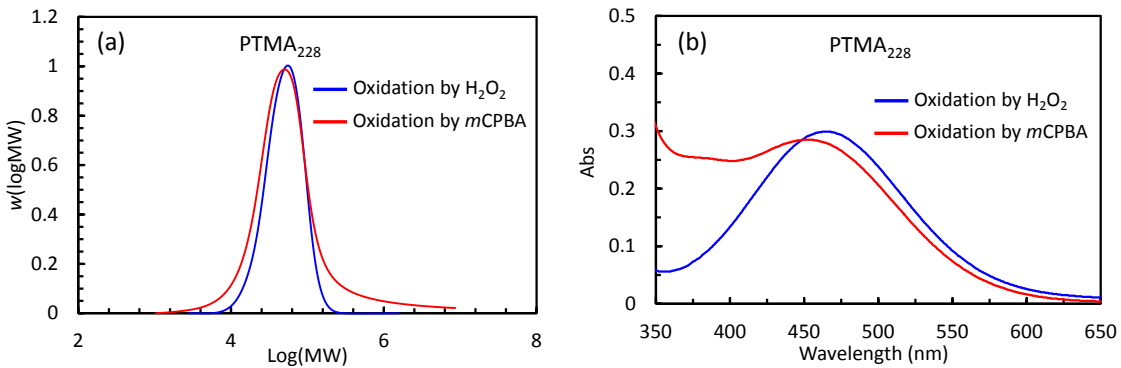


Figure S5. Comparison of two different oxidation methods to convert PTMPM₂₂₈ to PTMA₂₂₈, (a) SEC traces and (b) the UV-Vis spectra of PTMA₂₂₈ oxidised by H_2O_2 in methanol and $mCPBA$ in dichloromethane.

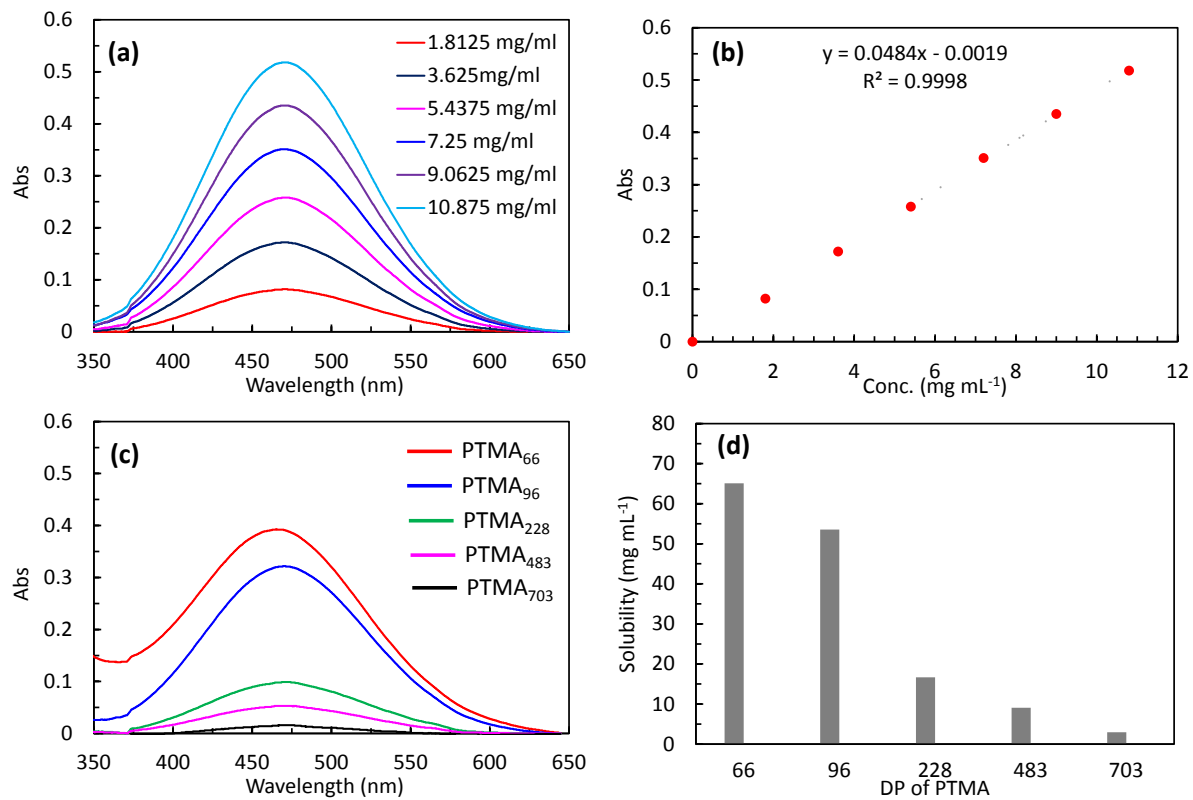


Figure S6. Solubility of PTMA in DMC with 1 M LiPF₆ determined by UV-Vis: (a) Absorption of 4-hydroxyl TEMPO with different concentration in THF, (b) Calibration curve (c) Absorption of PTMA in THF and (d) Solubility of PTMA with different DPs determined by UV-Vis.

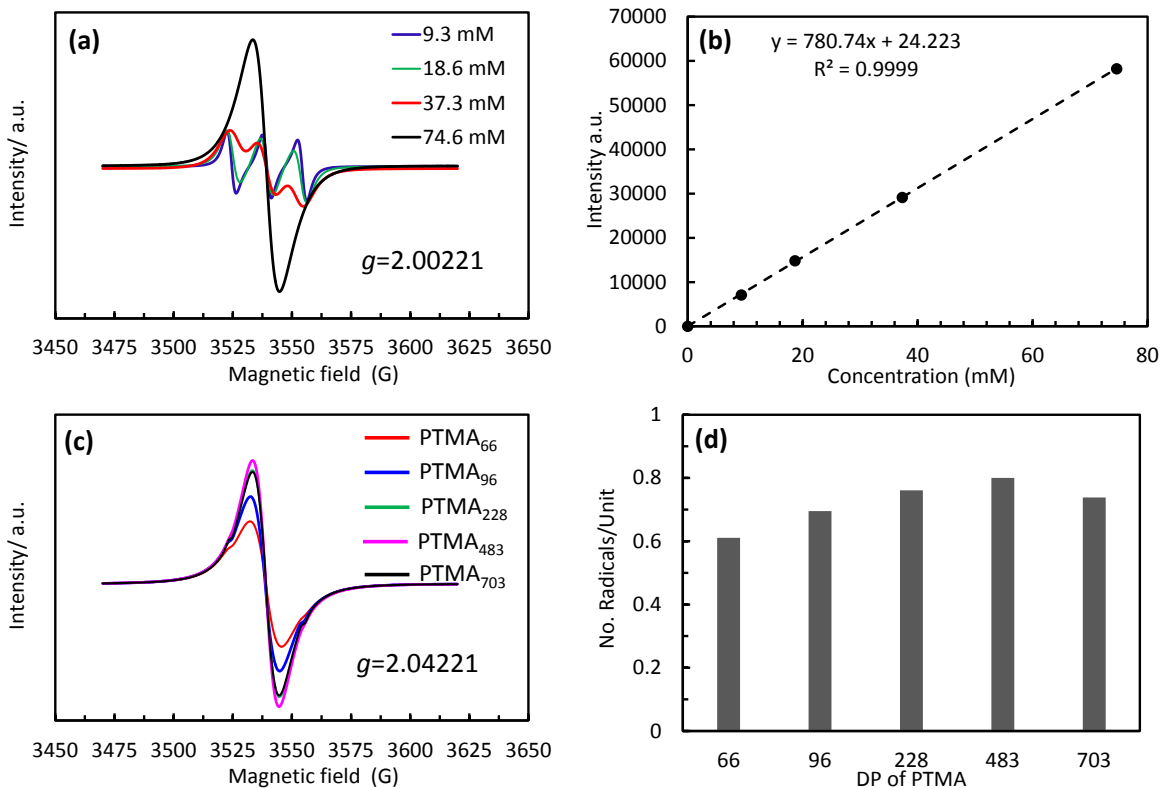


Figure S7. Oxidation efficiency determined by EPR: (a) EPR spectra of 4-hydroxyl TEMPO with different concentration in DCM, (b) Calibration curve based on integration of EPR spectra (c) EPR spectra of PTMA with different DPs oxidised from PTMPM by H₂O₂ and (d) Number of radicals per unit vs DP of PTMA determined by EPR.

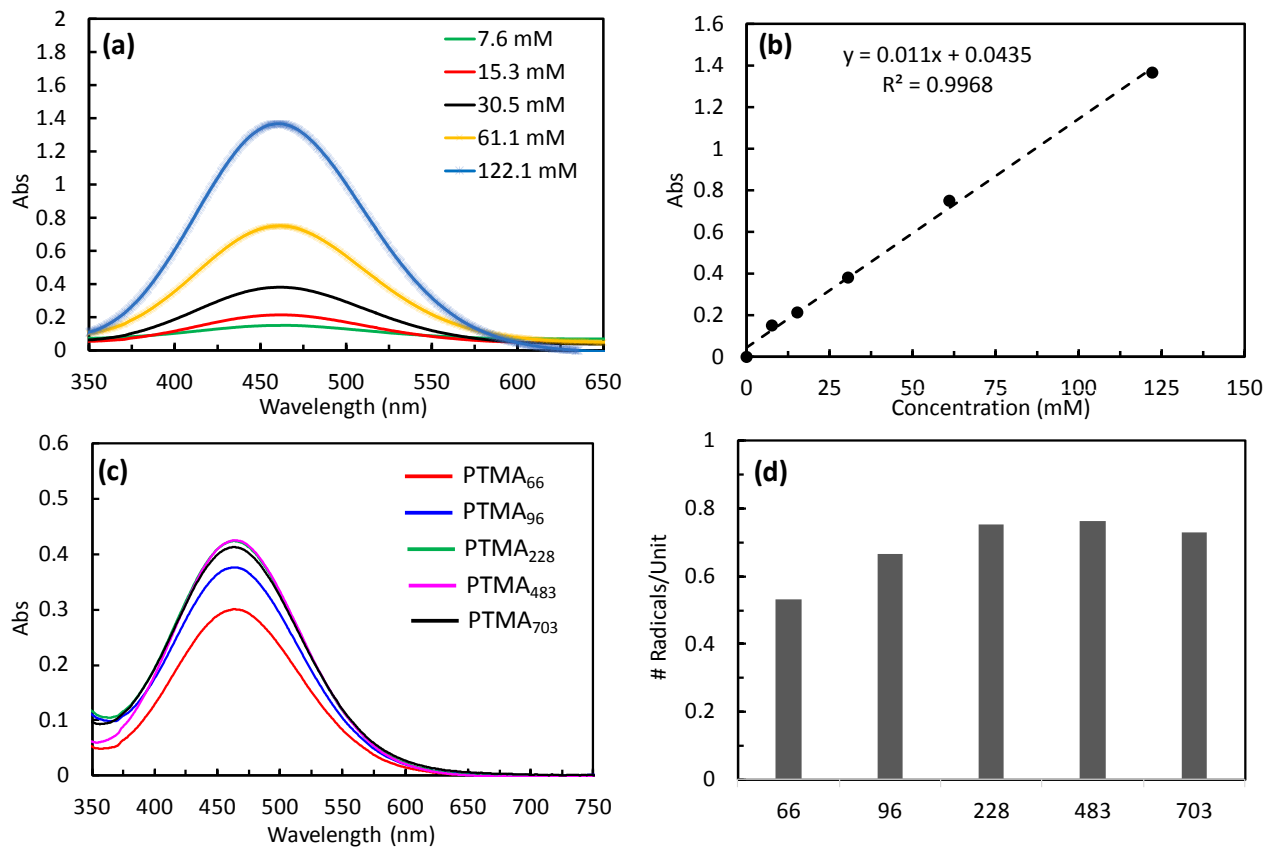


Figure S8. Oxidation efficiency determined by UV-Vis: (a) Absorption of 4-hydroxyl TEMPO with different concentration in DCM, (b) Calibration curve (c) Absorption of PTMA with different DPs oxidised from PTMPM by H₂O₂ and (d) Number of radicals per unit vs DP of PTMA determined by UV-Vis.

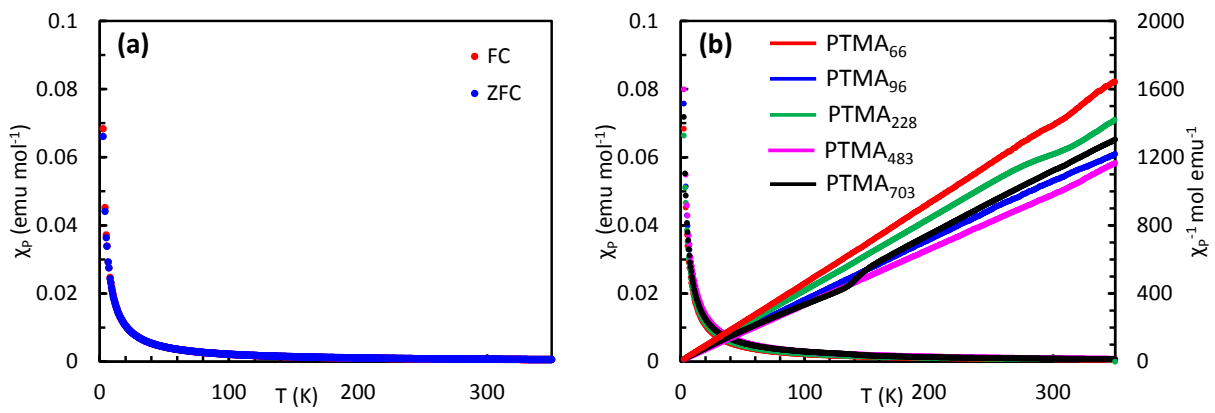


Figure S9. (a) Temperature dependence of the paramagnetic susceptibility χ_P of PTMA₆₆ with both field cooling (FC) and zero-field cooling (ZFC) modes. (b) Temperature dependence of the paramagnetic susceptibility χ_P and its inverse χ_P^{-1} of all PTMA polymers with FC mode. All the measurements carried out at an applied magnetic field strength of 10 KOe.

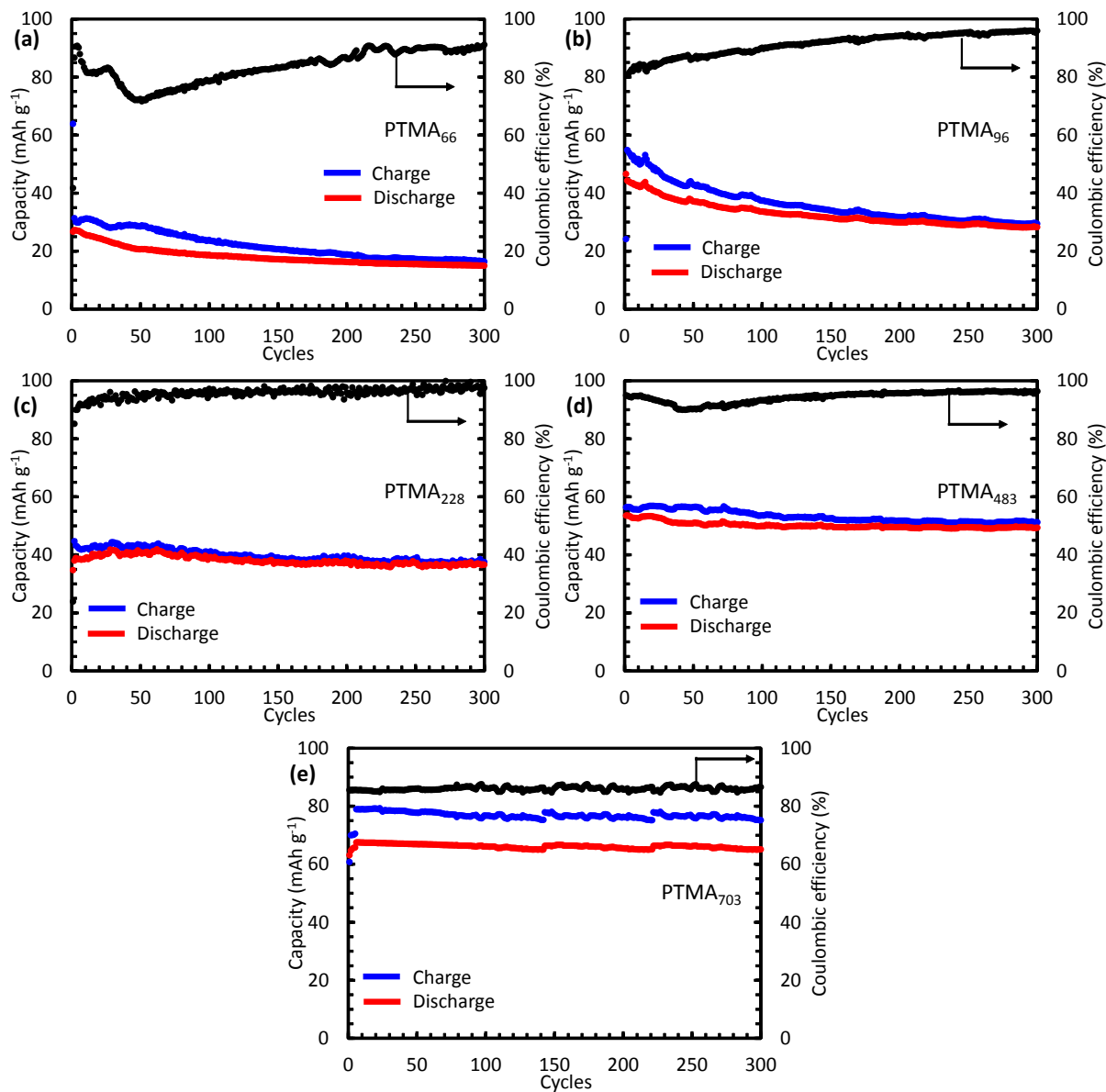


Figure S10. Cycling property and coulombic efficiency of (a) PTMA₆₆, (b) PTMA₉₆, (c) PTMA₂₂₈, (d) PTMA₄₈₃, and (e) PTMA₇₀₃ as cathode with mass ratio of PTMA/SP carbon/PVdF=0.25/0.65/0.1, charging/discharging at 1C over 300 cycles.

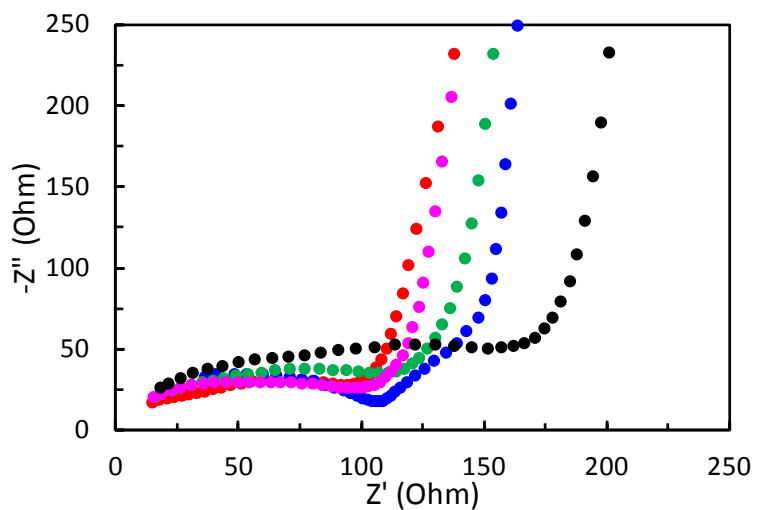


Figure S11. Nyquist plot of PTMA with different DPs as cathode at mass ratio of PTMA/SP carbon/PVdF=0.25/0.65/0.1, and 0.1 M LiPF₆ in DMC as electrolyte.